EUKARYOTIC CELL, Aug. 2006, p. 1314–1327 Vol. 5, No. 8
1535-9778/06/$08.00+0 doi:10.1128/EC.00386-05


# Import-Associated Translational Inhibition: Novel In Vivo Evidence for Cotranslational Protein Import into *Dictyostelium discoideum* Mitochondria

Afsar U. Ahmed,[1] Peter L. Beech,[2] Sui T. Lay,[1] Paul R. Gilson,[2] and Paul R. Fisher[1]*

*Department of Microbiology, La Trobe University, Victoria 3086,[1] and Centre for Cellular and Molecular Biology, School of Biological and Chemical Sciences, Deakin University, Victoria 3125,[2] Australia*

Received 27 December 2005/Accepted 29 May 2006

**To investigate protein import into the mitochondria of *Dictyostelium discoideum*, green fluorescent protein (GFP) was fused as a reporter protein either to variable lengths of the N-terminal region of chaperonin 60 (the first 23, 40, 80, 97, and 150 amino acids) or to the mitochondrial targeting sequence of DNA topoisomerase II. The fusion proteins were expressed in AX2 cells under the actin-15 promoter. Fluorescence images of GFP transformants confirmed that *Dictyostelium* chaperonin 60 is a mitochondrial protein. The level of the mitochondrially targeted GFP fusion proteins was unexpectedly much lower than the nontargeted (cytoplasmic) forms. The distinction between targeted and nontargeted protein activities was investigated at both the transcriptional and translational levels in vivo. We found that targeting GFP to the mitochondria results in reduced levels of the fusion protein even though transcription of the fusion gene and the stability of the protein are unaffected. [$^{35}$S]methionine labeling and GFP immunoprecipitation confirmed that mitochondrially targeted GFP is translated at much slower rates than nontargeted GFP. The results indicate a novel phenomenon, import-associated translational inhibition, whereby protein import into the mitochondria limits the rate of translation. The simplest explanation for this is that import of the GFP fusion proteins occurs cotranslationally, i.e., protein synthesis and import into mitochondria are coupled events. Consistent with cotranslational import, Northern analysis showed that the GFP mRNA is associated with isolated mitochondria. This association occurred regardless of whether the GFP was fused to a mitochondrial leader peptide. However, the presence of an import-competent leader peptide stabilized the mRNA-mitochondria association, rendering it more resistant to extensive EDTA washing. In contrast with GFP, the mRNA of another test protein, aequorin, did not associate with the mitochondria, and its translation was unaffected by import of the encoded polypeptide into the mitochondria.**

Most mitochondrial proteins are encoded by the nuclear genome and synthesized in the cytoplasm prior to their import into the organelle. Mitochondrial preproteins can traverse either one or both mitochondrial membranes to reach their final destination in one of the four subcompartments: the outer membrane, the intermembrane space, the inner membrane, and the matrix. These preproteins possess a specific targeting sequence that generally resides at the N terminus, called the presequence, which is essential for recognition by the mitochondrial import apparatus and is removed upon import by mitochondrial-processing peptidase in the matrix. Mitochondrial presequences do not share any primary sequence identity, but they are enriched in positively charged, hydroxylated, and hydrophobic amino acids and have the ability to form an amphiphilic α-helix. In a helical wheel projection, the positively charged amino acids localize on one side of the helix, while the opposite side is uncharged and hydrophobic (36, 37, 42). This amphiphilic α-helical structure is critical for mitochondrial import, as Tom20, a component of the TOM complex (*t*ranslocase in the *o*uter *m*itochondrial membrane), recognizes the hydrophobic surface and Tom22 recognizes the hydrophilic surface (3). The energy for protein translocation through the mitochondrial membranes is provided by the membrane potential across the mitochondrial inner membrane and ATP (34).

The mitochondrial import apparatus is a very dynamic, multisubunit system that has been extensively studied over the past years (33), but the mechanism of preprotein delivery to the mitochondria is not well understood. One of the open questions concerning mitochondrial protein import is whether import is initiated during or after the completion of protein synthesis in the cytosol, i.e., whether protein import into mitochondria occurs in a cotranslational or posttranslational manner. The mechanism of mitochondrial protein import has been extensively studied using in vitro import reactions, and according to in vitro observations, most mitochondrial proteins can be successfully imported posttranslationally (15, 25). Furthermore, disruption of the mitochondrial membrane potential in vivo can result in accumulation of proteins that are able to be imported into mitochondria following the reestablishment of the membrane potential. This shows that translation and import are not necessarily coupled (35).

However, several lines of evidence suggest the involvement of cotranslational protein import at least for some mitochondrial proteins (40, 24). Firstly, after cycloheximide-induced translational arrest in yeast cells, ribosomes synthesizing mitochondrial proteins were found associated with isolated mito-

* Corresponding author. Mailing address: Department of Microbiology, Thomas Cherry Building, La Trobe University, Bundoora, Victoria 3086, Australia. Phone: 61 3 9479 2229. Fax: 61 3 9479 1222. E-mail: fisher@lumi.latrobe.edu.au.

chondria (18–20). Secondly, under normal growth conditions, unprocessed mitochondrial precursor proteins are usually not detectable in yeast cells, and mitochondrial protein import can be instantaneously stopped by the inhibition of protein synthesis (1, 7, 8). Thirdly, methotrexate, an antifolate reagent, was able to block the import of a fusion protein consisting of the mitochondrial targeting signal of yeast cytochrome oxidase subunit IV fused to the mouse dihydrofolate reductase (DHFR) in vitro but not in vivo. This indicates that full-length precursor proteins do not exist in the cytosol in vivo and that, therefore, protein synthesis and import are very tightly coupled (7). In contrast, another study reported that aminopterine binding to a DHFR fusion with cytochrome $b_2$ arrested the import of up to 80% of the fusion protein in vivo in yeast cells (44). This result suggested posttranslational import for a major proportion of the DHFR fusion proteins and left open the possibility of cotranslational import for the remainder. Thus, the available evidence suggests that in vivo, cotranslational as well as posttranslational protein import into mitochondria can occur.

Recently, in both mammalian and yeast cells, the nascent polypeptide chains destined for mitochondria were reported to be associated with a complex in the cytosol, called the nascent polypeptide-associated (NAC) complex (43, 11). Subunits of both the NAC complex and its homologue, the ribosome-associated complex (10), are required for normal mitochondrial protein import, suggesting that they play an active role in targeting the complexes to the vicinity of the mitochondria (9, 11) and that the nascent peptides need to be in the vicinity of the mitochondria for efficient sorting of proteins into the organelles. Not only are nascent mitochondrial polypeptides targeted to the mitochondria but also the specific mRNAs for at least some proteins appear to have *cis*-acting signals which direct their translocation to the mitochondrial surface (17, 38). For example, the 5′ N-terminal coding region and 3′ untranslated region (UTR) of ATM1 mRNA contain *cis*-acting signals which can direct heterologous RNA molecules to the mitochondria in vivo, and this mRNA targeting is independent of the translation of 5′ sequence (5, 26). As a result, mRNA targeting to the vicinity of the mitochondria can be regarded as a prerequisite for cotranslational protein import into mitochondria.

Overall, the reports on cotranslational protein import mainly support the biological existence of this import mechanism at least for some mitochondrial proteins. In this paper, we report the first in vivo studies of mitochondrial protein import in the social amoeba *Dictyostelium discoideum*. Using green fluorescent protein (GFP) as a reporter, we found that translation of mitochondrially targeted GFP fusion proteins is limited by the process of mitochondrial protein import. This novel phenomenon of import-associated translational inhibition suggests that GFP import is cotranslational, a hypothesis supported by the finding that GFP mRNA is associated with isolated mitochondria. The translation of another test protein, aequorin, was found, by contrast, to be unaffected by import into the mitochondria, and the aequorin mRNA did not associate with the mitochondria. The results suggest that whether or not a polypeptide is imported cotranslationally into the mitochondria depends upon whether or not its encoding mRNA is transported to the mitochondrial surface.

## MATERIALS AND METHODS

**Construction of GFP and aequorin fusion genes by spliced overlap extension PCR.** The GFP coding region and variable lengths of the chaperonin 60 N-terminal region were amplified by the PCR from the corresponding cDNA clones, pA15GFP (6) and pPROF129 (23), respectively. In the primary PCR, cDNA synthesis was carried out using gene-specific primers designed to amplify various lengths (which encode the first 23, 40, 80, 97, and 150 amino acids) of the chaperonin 60 N-terminal coding sequence. The amplified fragments were fused in frame at the 3′ end with 38 bp of the GFP N-terminal coding sequence that had been incorporated into the 3′ end primer. Similarly, gene-specific primers were also used to amplify the full-length GFP coding sequence (0.7 kb) fused in frame at the 5′ end with primer-incorporated 30 to 33 bp of the 3′ end of variable lengths of the chaperonin 60 N terminus. Specific primers used to generate these PCR products are listed in Table 1. In the secondary PCR, both the PCR-amplified chaperonin 60 N-terminal fragment and the full-length GFP coding sequence with corresponding overlapping regions were used together as templates to amplify the final fusion gene. A GFP fusion with the first 82 amino acids of *Dictyostelium* mitochondrial DNA topoisomerase II (*topA*) was constructed in a similar manner using a cDNA clone (pTOPA-1) (22) to amplify the TopA N-terminal sequence. Amplifications were carried out for 35 cycles with standard denaturation, annealing, and extension temperatures (94, 60, and 72°C, respectively), with various extension times depending on the size of the target sequence. Restriction enzyme recognition sites of EcoRI, ClaI, and XhoI (Table 1) were incorporated into primers to obtain the final fusion product with EcoRI-ClaI (5′ end) and XhoI-EcoRI (3′ end) sites for cloning purposes. After gel purification, the final PCR products were cloned into the EcoRI site of pZErO-2 (Invitrogen) and verified by sequencing. Finally, the fusion products were subcloned between the ClaI and XhoI sites of the *Dictyostelium* expression vector pA15GFP, where they replaced the original GFP gene. The resulting constructs were designated pPROF294 (expressing Cpn23.GFP), pPROF295 (expressing Cpn40.GFP), pPROF296 (expressing Cpn80.GFP), pPROF297 (expressing Cpn97.GFP), pPROF298 (expressing Cpn150.GFP), and pPROF299 (expressing TopA82.GFP). In each of them, the expression and termination of the fusion gene are regulated by the *Dictyostelium* actin-15 promoter and actin-8 transcription terminator, respectively. The vector backbone contains a G418 resistance marker expressed under the actin-6 promoter. In a similar fashion, aequorin fusion constructs were made using the chaperonin 60 N-terminal coding sequences (the first 23, 40, and 150 amino acid coding sequences), an N-terminal sequence of *topA* (the first 82-amino-acid coding sequence), and an N-terminal sequence of *Dictyostelium* mitochondrial nucleoside diphosphate kinase (*ndkM*) (39) (the first 60-amino-acid coding sequence).

**Transformation and cell culture.** The transformation of *Dictyostelium* wild-type strain AX2 with the constructed plasmids was carried out as previously described (30). Individual clones were purified by streaking on *Klebsiella aerogenes* lawns on nutrient (SM) agar containing 20 μg/ml G418 and then grown in 24-well Costar plate wells (Nunc) containing 0.8 ml HL5 growth medium supplemented with antibiotics (20 μg/ml G418, 100 μg/ml ampicillin, 25 μg/ml kanamycin, 10 μg/ml streptomycin, and 5 μg/ml tetracycline). Axenic growth of larger volumes of the transformants was carried out at 21°C in antibiotic-supplemented HL5 medium on an orbital shaker (150 rpm). For growth on bacterial lawns, individual transformants were grown with *Klebsiella aerogenes* on G418-supplemented SM agar plates at 21°C, and the vegetative amoebae were harvested from the clearing lawn in ice-cold sterile saline by washing four times at 3,000 × *g* for 30 s to eliminate bacteria.

**Growth experiments (determination of the generation times).** Growth experiments were carried out with axenic culture of *Dictyostelium* cells in HL5 medium without antibiotics. During axenic growth, cell numbers were counted every 10 to 12 h using a hemocytometer. Generation times were determined by linear regression analysis of the logarithm of the cell counts during exponential growth versus time. The regression analysis was conducted in R (The R Project for Statistical Computing, http://www.r-project.org/), a free software implementation of S, an environment for statistical computing and graphics (4).

**Fluorescence microscopy.** Fluorescence microscopy of *Dictyostelium* cells expressing GFP was performed according to the procedure described previously (13) with the following modifications. Briefly, following the growth of the vegetative amoebae up to log phase in HL5 media on sterile coverslips in six-well plates (Nunc), the mitochondria were labeled with 100 nM MitoTracker Red (CMX-Ros; Invitrogen Molecular Probes) in LoFlo HL5 (3.85 g/liter glucose, 1.78 g/liter Proteose peptone, 0.45 g/liter yeast extract, 0.485 g/liter $KH_2PO_4$, and 1.2 g/liter $Na_2HPO_4 \cdot 12H_2O$; filter sterile) for 1 h. LoFlo HL5 was used to reduce autofluorescence from the HL5 medium. Unbound MitoTracker Red was removed by washing the cells three to four times in LoFlo HL5 over 2 h. After washing the coverslips twice in phosphate buffer (12 mM $Na_2HPO_4$, 12 mM

TABLE 1. Primers used in this study to generate GFP and aequorin fusion constructs

| Primer[a] | Sequence (5′–3′)[b] |
|---|---|
| Cpn60 (forward) | GCGGAATTCATCGATGCTTGGACCGAAAAAAACAAAATGTTTAGACAAATTGC |
| Cpn23.GFP (reverse) | GGGACAACTCCAGTGAAAAGTTCTTCTCCTTTACTCATAATATCTTTACCAGTTGAATAATTTCTTAATCC |
| Cpn40.GFP (reverse) | GGGACAACTCCAGTGAAAAGTTCTTCTCCTTTACTCATTAATTGTTCAACACCACGTAACATTAATGC |
| Cpn80.GFP (reverse) | GGGACAACTCCAGTGAAAAGTTCTTCTCCTTTACTCATAGCAAATTCAATATGTTTAGCGACAGTAACACC |
| Cpn97.GFP (reverse) | GGGACAACTCCAGTGAAAAGTTCTTCTCCTTTACTCATCCTTGAAGCAACACCTTTAACTAATTGAGCACC |
| Cpn150.GFP (reverse) | GGGACAACTCCAGTGAAAAGTTCTTCTCCTTTACTCATGGTTTTAAGTTCACCAACAACTTTTTCAACTGC |
| TopA82.GFP (reverse) | GGGACAACTCCAGTGAAAAGTTCTTCTCCTTTACTCATTGTTTTTTCTGATATTTTTTC |
| Cpn23.GFP (forward) | GGATTAAGAAATTATTCAACTGGTAAAGATATTATGAGTAAAGGAGAAGAACTTTTCACTGGAGTTGTCCC |
| Cpn40.GFP (forward) | GCATTAATGTTACGTGGTGTTGAACAATTAATGAGTAAAGGAGAAGAACTTTTCACTGGAGTTGTCCC |
| Cpn80.GFP (forward) | GGTGTTACTGTCGCTAAACATATTGAATTTGCTATGAGTAAAGGAGAAGAACTTTTCACTGGAGTTGTCCC |
| Cpn97.GFP (forward) | GGTGCTCAATTAGTTAAAGGTGTTGCTTCAAGGATGAGTAAAGGAGAAGAACTTTTCACTGGAGTTGTCCC |
| Cpn150.GFP (forward) | GCAGTTGAAAAAGTTGTTGGTGAACTTAAAACCATGAGTAAAGGAGAAGAACTTTTCACTGGAGTTGTCCC |
| TopA82.GFP (forward) | GAAAAAATATCAGAAAAAACAATGAGTAAAGGAGAAGAACTTTTCACTGGAGTTGTCCC |
| GFP (reverse) | GCGGAATTCCTCGAGTTATTTGTATAGTTCATCCATGCCATGTGTAATCCC |
| TopA (forward) | GCGGATTCATCGATATGTCAAAATTATTAAATAATAATAATCATAAAAATTTAACAAATTATTAAAAATTTGG |
| Ndk (forward) | GCGGATTCATCGATAAAATGTTCTCAAGATTTGCTCGTGC |
| Cpn23.Aeq (reverse) | GCTTGACTGAGTATTGTTCGCTGGTCATAATATCTTTACCAGTTGAATAATTTCTTAATCC |
| Cpn40.Aeq (reverse) | GCTTGACTGAGTATTGTTCGCTGGTCATTAATTGTTCAACACCACGTAACATTAATGC |
| Cpn150.Aeq (reverse) | GCTTGACTGAGTATTGTTCGCTGGTCATGGTTTTAAGTTCACCAACAACTTTTTCAACTGC |
| TopA82.Aeq (reverse) | GCTTGACTGAGTATTGTTCGCTGGTCATTGTTTTTTCTGATATTTTTTC |
| Ndk60.Aeq (reverse) | GCTTGACTGAGTATTGTTCGCTGGTCATCCTAGGCTCTTGAGTCGACTTATTTTC |
| Cpn23.Aeq (forward) | GGATTAAGAAATTATTCAACTGGTAAAGATATTATGACCAGCGAACAATACTCAGTCAAG |
| Cpn40.Aeq (forward) | GCATTAATGTTACGTGGTGTTGAACAATTAATGACCAGCGAACAATACTCAGTCAAG |
| Cpn150.Aeq (forward) | GCAGTTGAAAAAGTTGTTGGTGAACTTAAAACCATGACCAGCGAACAATACTCAGTCAAG |
| TopA82.Aeq (forward) | GAAAAAATATCAGAAAAAACAATGACCAGCGAACAATACTCAGTCAAG |
| Ndk60.Aeq (forward) | GAAAATAAGTCGACTCAAGAGCCTAGGATGACCAGCGAACAATACTCAGTCAAG |
| Aeq (reverse) | GCGGAATTCCTCGAGTTAGGGGACAGCTCCACCGTAGAGCTTTTCGC |

[a] Cpn60, chaperonin60 (*hspA*); Ndk, nucleoside diphosphate kinase (*ndkM*); Ndk60, the first 60-amino-acid coding sequence of *ndkM*. All forward primers are 5′ primers and all reverse are 3′ primers. For example, Cpn23.GFP (reverse) primer is the 3′ primer to amplify the first 23-amino-acid coding sequence of chaperonin 60 fused in frame at the 3′ end with the first 38 bp of the GFP coding sequence, whereas Cpn23.GFP (forward) is the 5′ primer to amplify the full coding sequence of GFP fused in frame at the 5′ end with the 3′ end of the first 23-amino-acid coding sequence of chaperonin 60.

[b] Restriction enzyme recognition sites, underlined in Cpn60 (forward) and GFP (reverse), are EcoRI-ClaI (5′–3′) and EcoRI-XhoI (5′–3′), respectively. Sequences in boldface type are of *hspA* (chaperonin 60); double underlined and highlighted sequences belong to *topA* and *ndkM*, respectively.

$NaH_2PO_4$ [pH 6.5]), cells were fixed and flattened at the same time by placing the coverslips upside down on a layer of 1% agarose in phosphate buffer containing 3.7% paraformaldehyde for 30 min. After fixation, the cells attached on the coverslips were washed four times (5 min each) in standard phosphate-buffered saline prior to permeabilization in prechilled (−20°C) methanol. The coverslips were then washed again four times in phosphate-buffered saline and mounted for microscopy.

**Fluorometry.** GFP fluorescence was measured quantitatively on suspensions of washed cells using a Turner Biosystems Modulus fluorometer with the blue module.

**Isolation of mitochondria.** Isolation of mitochondria on a small scale was carried out with around $10^7$ cells in an Eppendorf tube using the mitochondria isolation kit (Pierce) according to the supplier's instructions. For the isolation of mitochondria on a large-scale, *Dictyostelium* cells were grown axenically in 1 liter of culture. During the exponential growth phase, cells were harvested at 3,000 rpm for 5 min in a Sorvall GSA rotor and washed once with ice-cold sterile saline. The cell pellet was resuspended in 9 volumes of HBD buffer (5 mM $KPO_4$ [pH 7.5], 2 mM $MgCl_2$, 1 mM 2-mercaptoethanol) and kept on ice for 1 h with gentle shaking. Once the cells were swollen, as observed microscopically, they were homogenized by vortexing at high speed with 1/5 volume of glass beads (425 to 600 μm; Sigma) for 2 min or until most of the cells were broken (confirmed microscopically). Mannitol-sucrose buffer (2.5×; 0.525 M mannitol, 0.175 M sucrose, 5 mM Tris-HCl, 5 mM EDTA, 5 mM $MgCl_2$, pH 7.5) was added to the homogenized cells to a 1× concentration. The suspension of the broken cells was centrifuged at 3,000 rpm for 10 min in a Sorvall SS-34 rotor. The supernatant fraction was saved, and the homogenization procedure described above was repeated once with the pellet, followed by the centrifugation at 3,000 rpm for 10 min in a Sorvall SS-34 rotor. The supernatant fractions were combined and centrifuged at 15,000 rpm for 15 min (Sorvall SS-34 rotor) to sediment mitochondria. The crude mitochondrial pellet was washed once with mannitol-sucrose buffer and was further purified on a sucrose gradient as follows: it was resuspended in SHB buffer (250 mM sucrose, 20 mM HEPES, pH 7.5), overlaid on a discontinuous gradient of 60%, 45%, 28%, and 5% sucrose in SHB buffer, and centrifuged at 14,000 rpm overnight in a Beckman 50Ti rotor. Mitochondria were collected at the 28 to 45% interface, washed twice with excess SHB buffer, and kept in the same buffer as a thick suspension at −70°C until needed. In some experiments, the mitochondria were additionally washed three times at 4°C with an EDTA-containing buffer (30 mM Tris-Cl [pH 7.4], 10 mM EDTA, and 5 mM 2-mercaptoethanol) to release loosely bound mitochondrion-associated polysomes (5). Each wash was carried out by resuspending the mitochondria in the buffer, followed by a 10-min centrifugation at 12,000 × g. From the homogenization step onwards, all procedures were performed at 4°C.

**Northern hybridization.** Total and mitochondrion-associated RNA were extracted using the TRIZOL reagent according to the supplier's instructions (GIBCO BRL) from exponentially growing *Dictyostelium* cells and isolated mitochondria, respectively. For Northern hybridization, extracted RNA was fractionated on 1% agarose gel in either formaldehyde containing morpholinepropanesulfonic acid (MOPS) buffer or Tris-acetate-EDTA buffer and transferred onto a Hybond N+ nylon membrane (Amersham) using 20× SSC (1× SSC is 0.15 NaCl plus 0.015 M sodium citrate). Transferred RNA was hybridized at 42°C in the presence of 50% (vol/vol) formamide with digoxigenin (DIG)-labeled DNA probes (DIG; Boehringer Mannheim) and detected with alkaline phosphatase-conjugated anti-DIG antibody using nitroblue tetrazolium color detection (Roche). DNA probes for Northern hybridization were obtained by PCR amplification.

**SDS-PAGE and Western blot analysis.** Whole-cell and mitochondrial extracts were prepared in the sample buffer for sodium dodecyl sulfate-polyacrylamide gel electrophoresis (SDS-PAGE) and were resolved in a 12% gel using the Bio-Rad MiniProtean II apparatus. For Western analysis, SDS-PAGE gels were blotted onto a nitrocellulose membrane (Osmonics, Inc.) using the Bio-Rad Mini Trans-Blot electrophoretic transfer cell. Nitrocellulose membranes were probed with the following antibodies: rabbit polyclonal antibodies against GFP (1:5,000) (Invitrogen Molecular Probes), rabbit polyclonal antibodies against a synthetic peptide consisting of the first 18 amino acids of *Dictyostelium* chaperonin 60 precursor protein, which had been conjugated to keyhole limpet hemocyanin (1:5,000) (Mimotopes), and rabbit polyclonal antibodies against *Dictyostelium* succinate dehydrogenase subunit A (SdhA) (1:5,000). Immunoreactive bands were visualized with anti-rabbit immunoglobulin G coupled to horseradish peroxidase followed by detection using the AEC Chromogen (3-amino-9-ethylcarbazole in *N,N*-dimethyl formamide) kit (AEC-101; Sigma).

**[$^{35}$S]methionine labeling and immunoprecipitation of radiolabeled GFP.** *Dictyostelium* vegetative cells were harvested in log phase, and $3 \times 10^7$ cells were resuspended in 1 ml HL5. [$^{35}$S]methionine was added to the cell suspension to a final concentration of 0.6 mCi/ml (555 MBq/ml; Amersham Biosciences), and cells were radiolabeled for 3 h on an orbital shaker (150 rpm). At hourly intervals, an equal volume of cell suspension (~333 μl) was withdrawn and divided into two aliquots. For one aliquot, the total protein was extracted using the sample buffer for SDS-PAGE and was used to detect total radiolabeled proteins. The protein extraction from the second aliquot was carried out using NP-40 lysis buffer (50 mM Tris [pH 6.8], 120 mM NaCl, 0.5% NP-40, and protease inhibitors) and was used to immunoprecipitate GFP. For immunoprecipitation, after an overnight incubation at 4°C with rabbit polyclonal antibodies against GFP (Invitrogen Molecular Probes), the protein extract was further incubated with protein A-Sepharose (Sigma) for 2 h at 4°C. The Sepharose beads with attached GFP-antibody complexes were washed four times with a wash buffer (20 mM Tris [pH 8.0], 1 mM EDTA, 0.5% NP-40) supplemented with 0.9 M NaCl and once without NaCl. Finally Sepharose-attached antigen was subjected to SDS-PAGE analysis. Detection and quantification of the radioactive signals were carried out using a Storm PhosphorImager (Amersham Biosciences).

**In vivo stability of GFP fusion proteins.** From 100 ml of axenic culture of exponentially growing *Dictyostelium* cells, 9 ml was withdrawn to which dimethyl sulfoxide and sodium azide were added to final concentrations of 10% (vol/vol) and 0.2% (vol/vol), respectively, and mixed by inversion. This withdrawn sample was regarded as a control ($t = 0$ min) and kept at −20°C until needed for protein extraction (dimethyl sulfoxide serves as a cryoprotectant against lysis during freeze-thawing). Immediately, a freshly made cycloheximide (Sigma) stock solution (10 mg/ml) in HL5 medium was added to the axenically growing culture to a final concentration of 1 mg/ml. Following the addition of cycloheximide, a number of samples were taken from the axenic culture in an identical manner at the 5th, 10th, 20th, 60th, 90th, 120th, and 180th min after the addition of cycloheximide. Protein extraction from all samples and the subsequent Western analysis were performed as described above using rabbit polyclonal antibodies against GFP and the leader peptide.

## RESULTS

**Targeting chaperonin 60-GFP fusion proteins to the mitochondria: effect of varying the length of the chaperonin 60 N-terminal sequence.** To facilitate the import of GFP into mitochondria, we used N-terminal portions of *Dictyostelium* chaperonin 60, a nucleus-encoded mitochondrial protein (23). Most mitochondrial proteins are synthesized with N-terminal matrix-targeting presequences, which carry the information for mitochondrial recognition and import. A previous report predicted the mitochondrial targeting signal of *Dictyostelium* chaperonin 60 to be located at the N terminus, as the first 18 amino acids share a conserved structural motif for mitochondrial presequences: the ability to form a positively charged amphiphilic α-helix (23). Based on the consensus recognition sequence RX ↓ XS (41), a potential mitochondrial peptidase recognition site (RN ↓ YS) (Fig. 1B) was also predicted in the location of residues 15 to 18 with the cleavage site after residue 16 (23), while the web-based program MitoProt II 1.0a4 predicted a mitochondrial peptidase cleavage site at amino acid 18.

To identify the signal on chaperonin 60 that might be required for mitochondrial import, we therefore chose five truncated N-terminal regions (the first 23, 40, 80, 97, and 150 amino acids) to fuse with GFP and express in the *Dictyostelium* expression vector pA15GFP under the control of the actin-15 promoter. In parallel, an N-terminal region (the first 82 amino acids) of the mitochondrial DNA topoisomerase II (TopA) was also analyzed as a positive control (22). The constructs were used to transform *D. discoideum* AX2 cells, and the transformants were tested to determine the subcellular distribution of GFP using epifluorescence microscopy. These results (Fig. 1A) verified that the N terminus of chaperonin 60 harbors a targeting signal which is sufficient to direct the import of a passenger protein into mitochondria. However, the first 23 amino acids of chaperonin 60 were found insufficient to constitute a competent mitochondrial targeting signal for targeting GFP to the mitochondria, whereas the first 40 (or more) amino acids did provide a sufficient signal for targeting.

**Targeting GFP chimeric proteins to the mitochondria limits expression at the translational level.** Based on fluorescence microscopy, the total activity of mitochondrially targeted GFP fusion proteins was found to be significantly lower than that of cytoplasmic GFP, and surprisingly, this phenomenon was found consistent among all transformants and for all constructs. Under the fluorescence microscope, every cell in a population expressing cytoplasmic GFP fluoresced much more strongly and required much shorter exposure times than those expressing GFP targeted to the mitochondria (typical examples are shown in Fig. 2A). Fluorometry on suspensions of $5 \times 10^6$ cells/ml showed that cell lines expressing cytoplasmic GFP were 60- to 80-fold more fluorescent than those expressing mitochondrially targeted GFP (Fig. 2B).

The following possibilities were considered for the comparatively low fluorescence of the targeted forms of GFP: (i) reduced expression of the fusion genes, i.e., the production of mRNAs may be restricted or the degradation of the mRNAs may be enhanced due to unwanted effects of the extended leader sequence, (ii) translational inhibition, i.e., the synthesis of the targeted fusion proteins may be limited due to an interaction between the processes of translation and mitochondrial import (for such translational inhibition to occur, translation has to be coupled with mitochondrial import, i.e., cotranslational import), (iii) the targeted fusion proteins may have a high turnover rate compared to that of the nontargeted forms, due to either the presence of the extended leader peptide or physiological differences between the cytoplasmic and the intramitochondrial environment, or (iv) the additional amino acids of the leader peptide may interfere with the correct folding of mitochondrially targeted GFP fusion proteins. To investigate the foregoing possibilities, the distinction between targeted and nontargeted GFP was studied at both the transcriptional and translational levels. Figure 3A shows that the levels of GFP mRNA for targeted and nontargeted GFP do not correlate with the differences in GFP fluorescence. However, in Western analysis, the amount of GFP protein is significantly higher for the nontargeted than the targeted forms, and this correlates with their corresponding GFP fluorescence. These results exclude the possibility that reduced transcription is the reason for the low fluorescence of mitochondrially targeted GFPs and suggest instead that the reduced fluorescence of the targeted GFPs is due either to decreased levels of translation or to increased rates of turnover of the imported protein. We therefore tested whether mitochondrial GFP was turned over rapidly by examining its stability after cycloheximide-induced inhibition of protein synthesis. The targeted forms of GFP were also found to be highly stable in cycloheximide-treated cells, with only slight decreases in the amount of protein even after 3 h (Fig. 3B). The results were quite different when the same experiment was conducted on cells expressing Cpn23.GFP, the nontargeted form of GFP carrying the first 23 amino acids of chaperonin 60 at its N terminus. Figure 3C

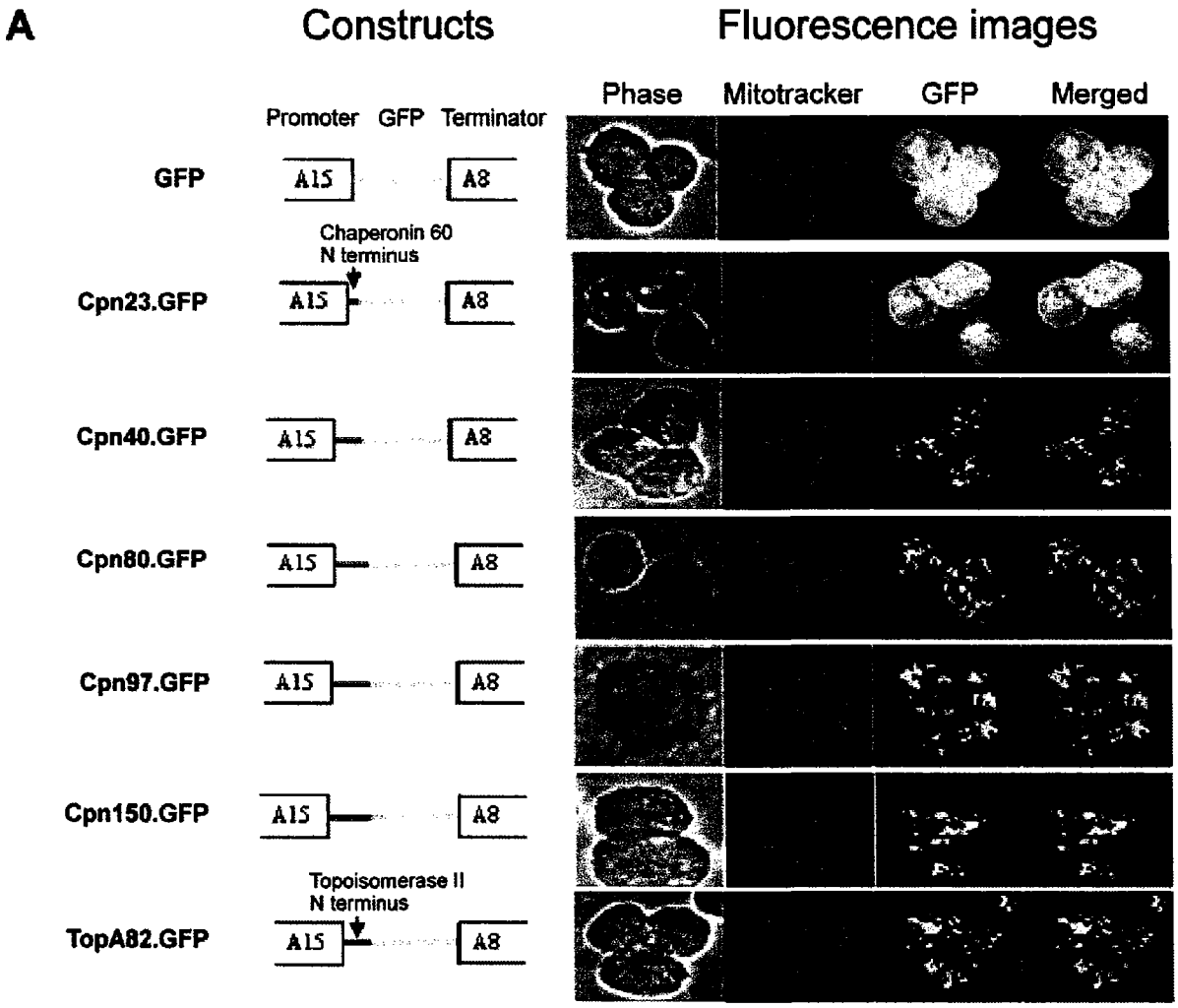


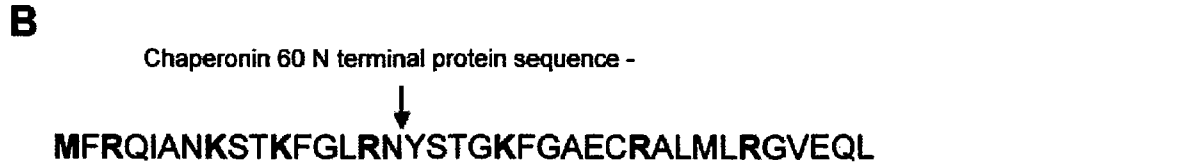


FIG. 1. (A) Subcellular distribution of GFP fusion proteins in *Dictyostelium discoideum* cells. The left panel shows the constructs of GFP fusion proteins. Except for GFP, which is a nontargeted, cytoplasmic control, six truncated versions of *Dictyostelium* mitochondrial proteins (coding sequences for the first 23, 40, 80, 97, and 150 amino acids of the N terminus of chaperonin 60 gene as well as the first 82 amino acids of DNA topoisomerase II) were fused at the 3′ end to the 5′ end of the GFP sequence (as described in Materials and Methods). These constructs were cloned into ClaI/XhoI sites of the *Dictyostelium* expression vector pA15GFP to facilitate expression under the actin-15 (A15) promoter and actin-8 (A8) terminator. The right panel shows the fluorescence microscopic images of *Dictyostelium* cells transformed (as described in Materials and Methods) with the corresponding constructs in the left panel. *Dictyostelium* transformants were grown in axenic media to log phase and were fixed on coverslips as described in Materials and Methods. The first column shows the phase-contrast images of the fixed *Dictyostelium* cells, followed by the MitoTracker Red (a mitochondrion-specific fluorescent dye; Invitrogen Molecular Probes) and GFP fluorescence images from the same sample. Mitochondrial localization of GFP was confirmed by the merged images (last column), where GFP fluorescence colocalized with that of MitoTracker Red. GFP fluorescence images for the transformants expressing GFP or Cpn23.GFP were taken with a 5-s exposure time, whereas longer exposure times (45 to 60 s) were required for the rest due to a lower intensity of GFP fluorescence. Exposure times for all MitoTracker Red images were within 5 s. (B) The first 40 amino acids of chaperonin 60 highlighting the positions of positively charged amino acids (boldface type) as well as a potential cleavage site (indicated by a downward arrow) as predicted initially based on consensus mitochondrial peptidase recognition site.

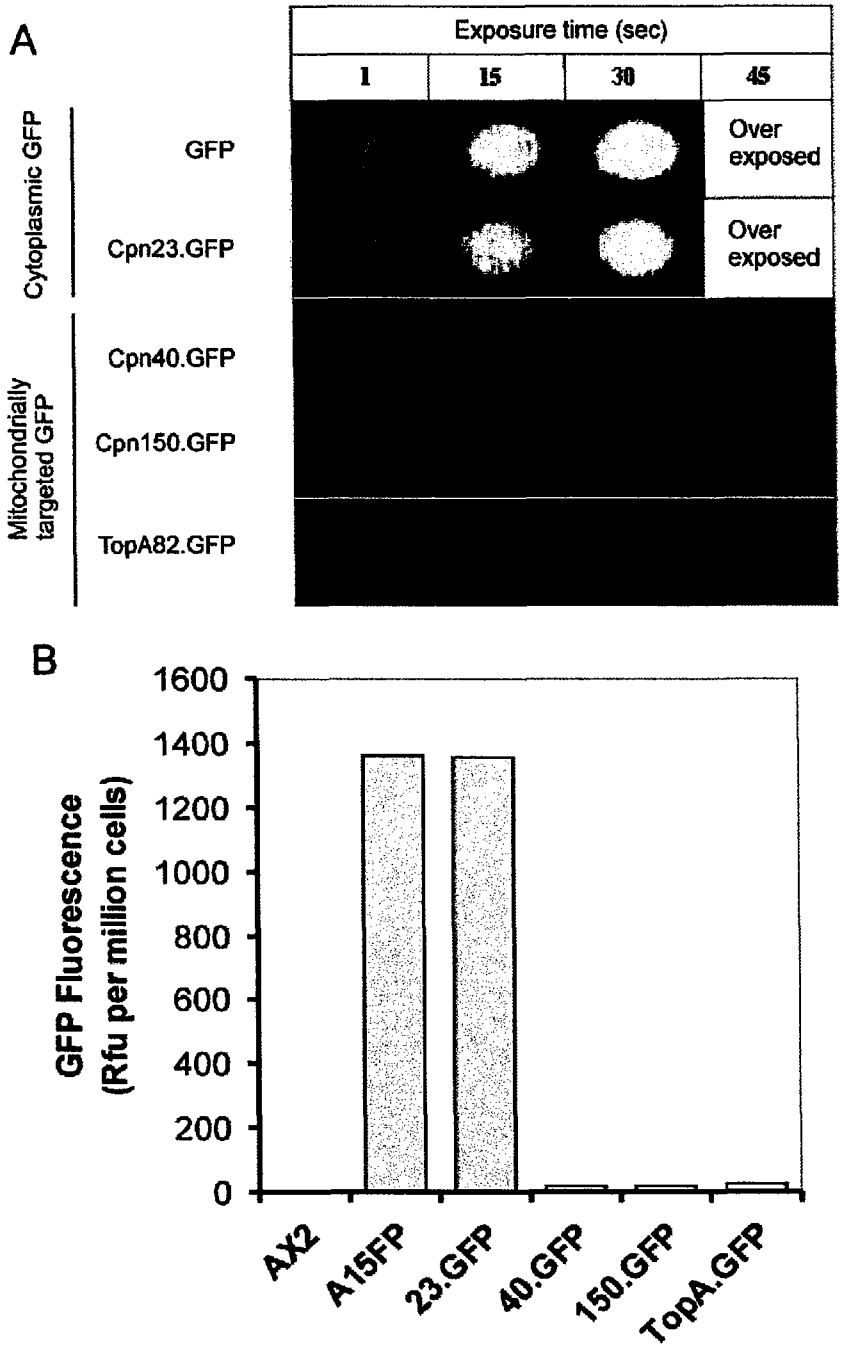


FIG. 2. (A) Mitochondrially targeted GFP fluorescence is much lower than that of cytoplasmic GFP. Microscopic images of GFP fluorescence were taken at variable exposure times (in seconds), as a measure of GFP activity, from a single *Dictyostelium* cell representative of the entire population of transformant cells. *Dictyostelium* transformants expressing either cytoplasmic or mitochondrially targeted GFP were grown to log phase in axenic media and were fixed on coverslips as described in Materials and Methods. Fixed cells were observed under a fluorescence microscope, and the images of GFP fluorescence were taken at variable exposure times (1, 15, 30, and 45 s). Cells expressing cytoplasmic GFP (GFP and Cpn23.GFP) were overexposed at 45 s (images not shown) due to much stronger GFP fluorescence than that of those expressing mitochondrially targeted GFP (Cpn40.GFP, Cpn150.GFP, and TopA82.GFP). (B) GFP fluorescence on transformant cell populations expressing either nontargeted (A15.FP and 23.GFP) or targeted (40.GFP, 150.GFP, and TopA.GFP) GFP fusion proteins. AX2 cells were used as a negative control. Axenically grown *Dictyostelium* cells were incubated with Lo-Flo HL5 for 2 h and then GFP fluorescence was measured in a fluorometer.

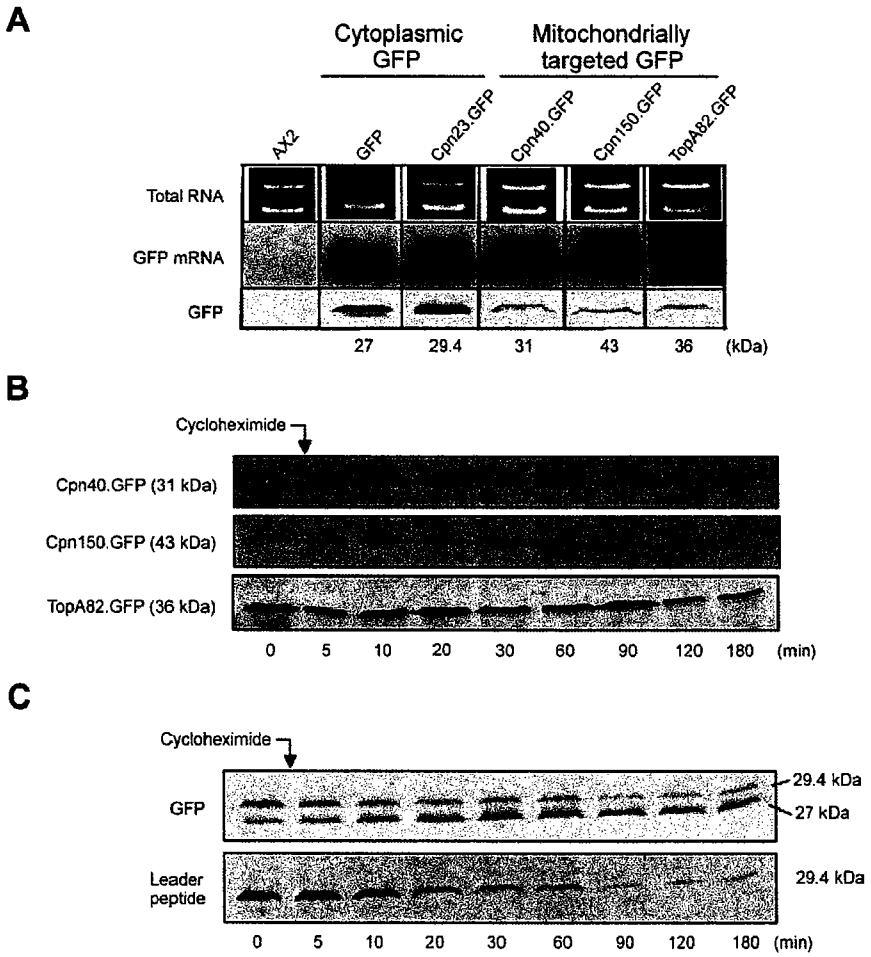


FIG. 3. Mitochondrially targeted GFP expression is limited at the translational level. (A) Targeted (mitochondrial) and nontargeted (cytoplasmic) GFP expression at both the protein and mRNA levels. Cells were harvested from bacterial lawns as described in Materials and Methods and were aliquoted for Northern and Western analysis (see Materials and Methods). All tracks in the SDS-PAGE gels were loaded with similar amounts of protein (22 to 24 μg). PCR-amplified GFP sequence was labeled with DIG as described in Materials and Methods and was used to detect the level of GFP mRNA in Northern analysis. In Western analysis, the level of GFP was detected with rabbit polyclonal anti-GFP (Invitrogen Molecular Probes), and the molecular masses of the observed bands are shown below. AX2 cells were used as negative controls in both Northern and Western analysis. (B) The stability of the mitochondrially targeted GFP fusion proteins was tested after cycloheximide-induced translational arrest as described in Materials and Methods. Briefly, aliquots of cells expressing mitochondrially targeted GFP were taken from axenic culture at log phase just before and at specific times (mentioned above) after the addition of cycloheximide to 1 mg/ml, and the level of GFP fusion proteins was detected with anti-GFP in Western analysis. (C) Stability of the nontargeted GFP fusion protein Cpn23GFP was tested after translational arrest induced by 1 mg/ml cycloheximide. Both the GFP itself and the leader peptide were detected in Western blots. Molecular masses are indicated on the left side of the blot.

shows that cells expressing Cpn23.GFP contain two GFP isoforms differing in apparent molecular mass by about 2.5 kDa. The use of a rabbit polyclonal antibody against the first 18 amino acids of the chaperonin 60 leader peptide (Mimotopes) revealed that only the larger isoform included the chaperonin 60 prepeptide. After protein synthesis was stopped by cycloheximide treatment, the leader peptide of this nontargeted GFP was gradually degraded and the larger GFP isoform gradually disappeared, and this was accompanied by a concomitant increase in the amount of the smaller isoform. By contrast, GFP itself was found to be quite stable, with only slight reductions in the amount of the smaller isoform by 3 h. These results are consistent with GFP's complete resistance to in vitro proteolytic degradation (unpublished data).

Cytosolic degradation of the leader peptide suggests that it is in an unfolded or partially unfolded state in the cytoplasm, whereas the GFP itself forms a tightly folded protease-resistant structure. Ni and coworkers reported similar cytosolic degradation of the aldehyde dehydrogenase leader peptide on enhanced GFP fusion proteins in HeLa cells (31). These authors found that inefficient import of the fusion protein due to mutations in the leader sequence resulted in cytosolic accumula-

tion of enhanced GFP lacking the mitochondrial leader peptide. The slow turnover of the leader peptide of Cpn23.GFP in the cytosol confirmed that the cycloheximide treatment had been effective in halting protein synthesis and in allowing detection of possible degradation of the GFP. The stability of the mitochondrially targeted GFP forms after cycloheximide treatment thereby rules out the possibility of high turnover rates as the explanation for low levels of the targeted proteins compared to the nontargeted forms.

**The rate of translation for the mitochondrially targeted GFP fusion proteins is limited.** The foregoing results showed that the levels of the targeted forms of GFP are constrained only at the translational level and suggest a reduced rate of translation for these targeted forms in vivo. To verify this directly, we measured the relative rates of translation in vivo of targeted and nontargeted forms of the GFP. Cells were labeled with [$^{35}$S]methionine, and GFP was immunoprecipitated at hourly intervals over the labeling period (see Materials and Methods). The relative rate of production of radiolabeled GFP during the labeling period was used as a measure of in vivo GFP translation rate. As shown in Fig. 4, the rate of radioactive Cpn23.GFP (nontargeted GFP) synthesis is much higher than that of either Cpn40.GFP or Cpn150.GFP (targeted GFPs). This was true regardless of whether the incorporation was measured relative to that for Cpn23.GFP after 3 h (Fig. 4A) or relative to the incorporation of radiolabel into total cellular protein (Fig. 4B). The rate of incorporation of radioactivity into total cellular protein in the whole-cell extract was quite comparable in the different cell lines (Fig. 4A, inset, and B, inset). We conclude that the rate of translation of mitochondrially targeted GFP is low compared to that of the cytosolic, nontargeted form.

**GFP mRNA is associated with isolated mitochondria, supporting evidence for cotranslational import.** During cotranslational import into mitochondria, the mRNA encoding the protein to be targeted must be associated with the mitochondrial surface. Other studies have suggested that, during cotranslational import into mitochondria, the mRNA encoding the protein to be targeted is localized on the mitochondrial surface as a part of the NAC complex (9, 11) or by means of *cis*-acting signals within the mRNA molecule (5, 26) Therefore, we determined whether GFP mRNA is associated with isolated mitochondria. In Northern analysis on isolated mitochondria, GFP mRNA was detected in all GFP transformants (Fig. 5A). As an internal loading and positive control, we probed for the small subunit rRNA (*rns*) of mitochondria (2). As a negative control for specificity of the GFP probe, we used RNA from isolated mitochondria of the parental nontransformed strain AX2. To eliminate the possibility of cytoplasmic mRNAs contaminating mitochondrial fractions as an artifact during the preparation of isolated mitochondria, we isolated mitochondria from a *Dictyostelium* cell line (HPF275) overexpressing a calcium-sensitive photoprotein, aequorin, in the cytoplasm (30). As shown in Fig. 5B, aequorin mRNA was detected in the whole-cell extract but not in the mitochondrial fraction.

Interestingly, GFP mRNAs encoding nontargeted proteins (pA15GFP and Cpn23.GFP) were also associated with mitochondria. Therefore, our results suggest that targeting of the GFP mRNA to the mitochondria does not depend upon the presence of a functional mitochondrial prepeptide in an al-

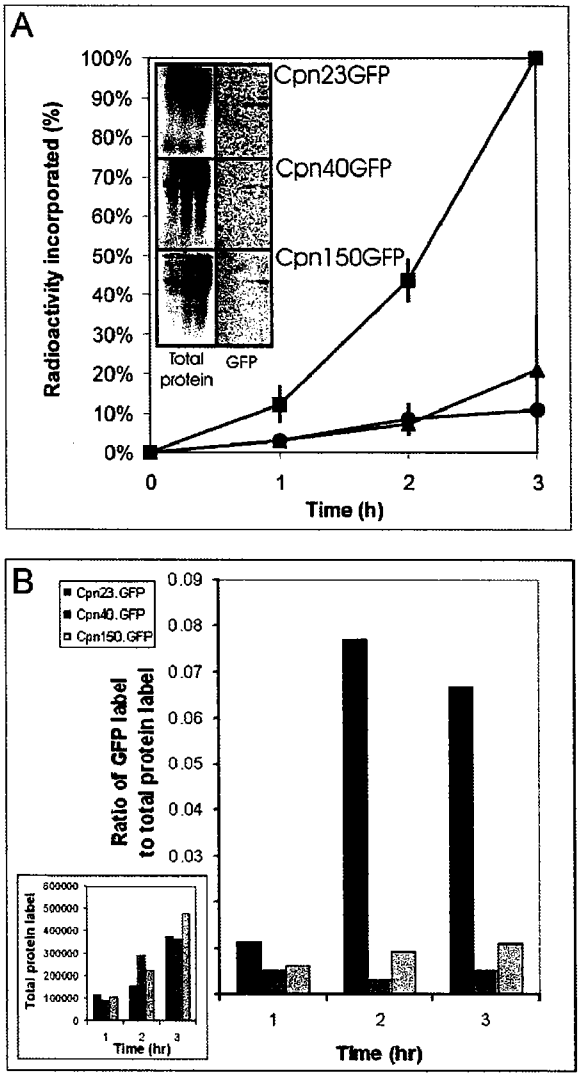


FIG. 4. The rate of GFP synthesis is higher for cytosolic than for mitochondrially targeted GFP. (A) Cells were labeled with [$^{35}$S]methionine for 3 h, and at hourly intervals, the incorporated radioactivity was detected in both the whole-cell extract and the immunoprecipitated GFP (see Materials and Methods). Radioactive signals were subjected to densitometric analysis using a Storm phosphorimaging system (Amersham Biosciences). In each experiment, the intensity of the radioactive GFP signal was normalized as a percentage of the maximum signal obtained (the Cpn23GFP signal at 3 h). The chart includes data from three independent experiments. Error bars represent standard errors of the mean. The inset shows the images of the radioactive signals from both the whole-cell extract and the immunoprecipitated GFP from one representative experiment. (B) Incorporation of radioactivity into immunoprecipitated GFP relative to the incorporation into total cellular protein. The inset shows the densitometric values for the total protein radioactive signal at hourly intervals. Negative controls using wild-type (AX2) cells (not expressing any GFP isoforms) showed similar levels of incorporation of radioactivity into total protein but no labeled GFP signal in immunoprecipitates (not shown).

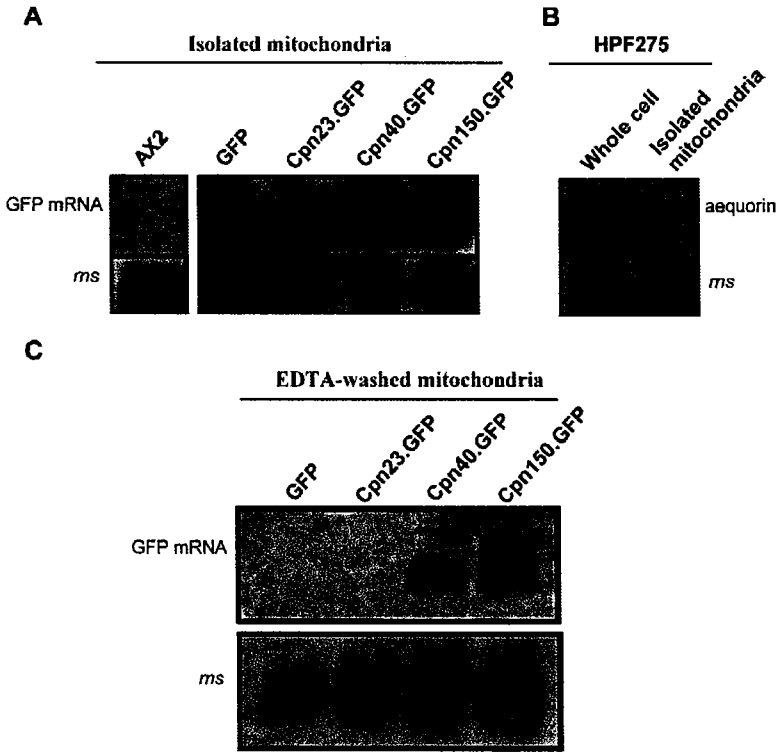


FIG. 5. Presence of GFP mRNA on the surface of mitochondria. (A) Mitochondria were isolated from AX2 cells as well as from all GFP transformants as described in Materials and Methods. RNA from the washed mitochondria was extracted and analyzed by Northern hybridization as described in Materials and Methods. Northern blots were hybridized with DIG-labeled probes for GFP (upper row) and the mitochondrial small subunit rRNA gene of *Dictyostelium* (2) (*rns*, lower row). (B) A *Dictyostelium* cell line (HPF275) overexpressing a calcium-sensitive photoprotein, aequorin, in the cytoplasm (30) was analyzed by Northern hybridization using a DIG-labeled aequorin or *rns* probe. The mitochondrial fraction from HPF275 was prepared as described in Materials and Methods. (C) A similar Northern analysis on the EDTA-washed mitochondria.

ready partially translated protein. This is consistent with previous reports showing that transport of mitochondrially targeted mRNA to the mitochondrial surface is independent of translation (17, 38).

The somewhat larger amounts of mitochondrially associated mRNA for the targeted GFPs suggested that translation and import of the targeted forms may stabilize the association of the mRNA with the mitochondrial surface. To investigate this possibility, we conducted further extensive washing of the mitochondria in the presence of EDTA. This treatment has been reported previously to release mitochondrion-bound polysomes (5). Although extensive EDTA washing reduced the GFP mRNA levels associated with the mitochondria of all transformants, the association for the mitochondrially targeted forms was relatively more resistant to this treatment than that of the nontargeted forms (Fig. 5C). The results suggest that GFP mRNA is transported to the mitochondria regardless of the presence of an import-competent leader peptide in the encoded protein but that the resulting association of the mRNA with the mitochondrial surface is stabilized by the leader peptide-dependent protein import process.

**The mRNA of mitochondrially targeted aequorin is not associated with the mitochondrial surface, and its translation is not limited by polypeptide import into the mitochondria.** In the preceding experiments, GFP mRNA was associated with the mitochondrial surface regardless of the presence or absence of a mitochondrial prepeptide in the encoded protein sequence. However, the presence of an import-competent prepeptide both stabilized the mRNA-mitochondrion association and limited the rate of translation. This raised the question of whether the presence of an import-competent mitochondrial leader peptide would be sufficient on its own to cause an association of the corresponding mRNA with the mitochondrial surface and produce import-associated translational inhibition. Aequorin presented itself as an ideal test protein to investigate this question, since the preceding experiments showed that, unlike GFP mRNA, the mRNA for cytosolic aequorin did not bind to the mitochondrial surface. We therefore made a series of constructs in which the aequorin coding sequence replaced that of GFP. Aequorin has a molecular mass of 22.5 kDa, close to that of GFP (27 kDa). The constructs were transformed into the same parental strain AX2. We confirmed by immunofluorescence microscopy (unpublished data) and by Western blotting using a rabbit polyclonal antibody against aequorin that the first 23 amino acids of chaperonin 60 were insufficient to target the aequorin to the mitochondria, while the longer prepeptides were import-competent, as was the case with GFP. Figure 6A shows that, as was the case with GFP, the expression

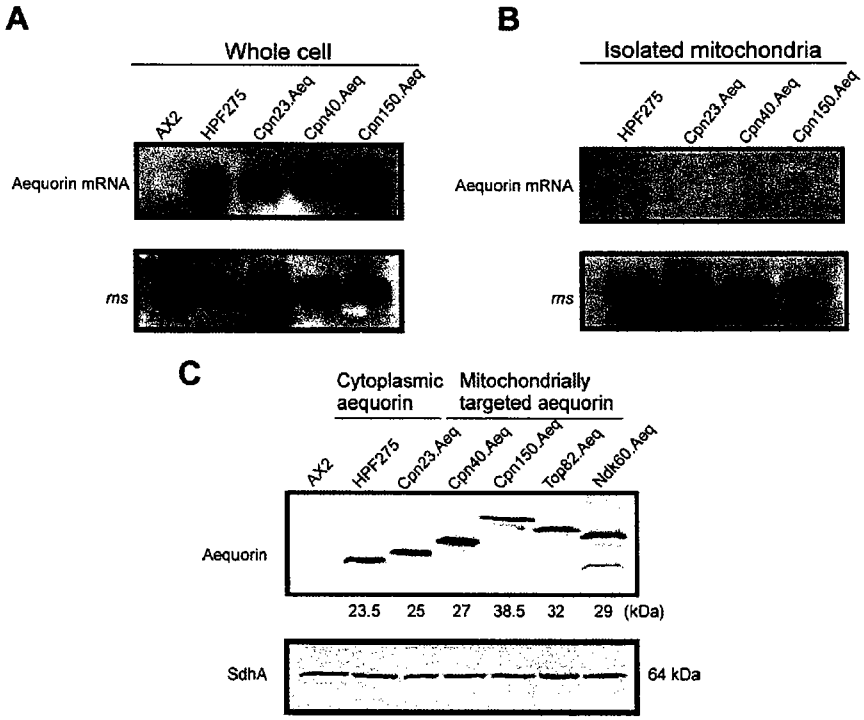


FIG. 6. Aequorin mRNAs are not associated with the mitochondria, and their translation is unaffected by mitochondrial import. (A) Northern analysis performed as described in Materials and Methods on the whole-cell extracts of AX2 cells and transformants expressing either cytoplasmic or mitochondrially targeted aequorin. A *Dictyostelium* cell line (HPF275) overexpressing aequorin in the cytoplasm (30) was used as a positive control for cytoplasmic aequorin. The level of aequorin mRNA was detected with the PCR-amplified aequorin sequence labeled with DIG as described in Materials and Methods, and the mitochondrial small subunit rRNA gene of *Dictyostelium* (2) (*rns*, lower row) was used as a loading control. (B) Similar Northern analysis performed on the mitochondria isolated from aequorin transformants. (C) Western analysis on whole-cell extracts of AX2 cells and transformants expressing either targeted or nontargeted aequorin. Ndk60.Aeq represents a transformant expressing a mitochondrially targeted aequorin fusion protein, where the first 60-amino-acid coding sequence of a precursor to *Dictyostelium* nucleoside diphosphate kinase was fused to the aequorin sequence by spliced-overlap PCR as described in Materials and Methods. The upper panel shows the level of GFP detected using an affinity-purified commercial polyclonal antibody against aequorin (AbCam), and the corresponding molecular masses were shown below. For SDS-PAGE, the whole-cell extracts were quantified using a Bio-Rad reagent according to the supplier's instructions, and similar amounts of proteins were loaded in each lane as shown by the level of SdhA as a loading control in the lower panel.

of aequorin mRNA was unaffected by whether or not the encoded polypeptide included an import-competent mitochondrial prepeptide. Unlike GFP mRNA, however, we failed to detect aequorin mRNA with isolated mitochondria even from those transformants expressing mitochondrially targeted aequorin (Cpn40.Aeq and Cpn150.Aeq) (Fig. 6B). These results suggest that, unlike GFP import, aequorin import into mitochondria is a posttranslational rather than a cotranslational process. In keeping with this conclusion, we did not observe any import-associated translational inhibition with the targeted forms of aequorin—the protein levels were quite similar for both targeted and nontargeted aequorin fusion proteins (Fig. 6C).

**Mitochondrially targeted GFPs do not interfere with the expression and import of other mitochondrial proteins.** The results in the preceding sections showed that the expression of mitochondrially targeted GFPs is limited at the translational level, suggesting that translation is coupled to and limited by import into the mitochondria. This raised the possibility that import of the mitochondrially targeted GFPs was stalling and potentially blocking or limiting the import not only of the GFPs but also of native mitochondrial proteins. If this were so, it would be reflected by the overall cell physiology and would adversely affect cellular growth rates. We therefore measured the generation times in HL5 medium of exponentially growing transformants expressing either targeted or nontargeted GFPs. In multiple growth experiments, all of the various transfor-

TABLE 2. Generation times of *Dictyostelium* transformants

| Transformant | GFP fusion protein | Generation time (h)[a] |
|---|---|---|
| AX2 | None | 12.5 (14.6, 10.9) |
| HPF611 | GFP | 11.0 (11.8, 10.3) |
| HPF612 | Cpn23.GFP | 11.4 (12.7, 10.4) |
| HPF613 | Cpn40.GFP | 11.5 (12.8, 10.5) |
| HPF614 | Cpn150.GFP | 12.0 (13.3, 10.9) |
| HPF615 | TopA82.GFP | 11.3 (13.4, 9.7) |

[a] The first figure of the generation time in each row represents the maximum likelihood estimate, and the values in parentheses represent the upper and lower 95% confidence limits.

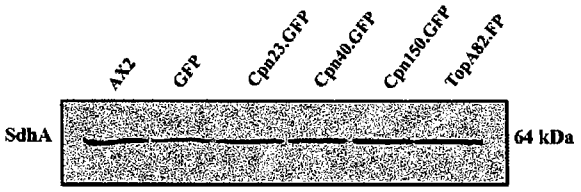


FIG. 7. Expression of *Dictyostelium* succinate dehydrogenase subunit A (SdhA) in wild-type and GFP transformants. *Dictyostelium* wild-type cells (AX2) and GFP transformants were grown axenically, and Western analysis was carried out with whole-cell extracts from log-phase cells using rabbit polyclonal antibodies against *Dictyostelium* succinate dehydrogenase subunit A (SdhA) as described in Materials and Methods. For SDS-PAGE, protein concentrations were measured using a Bio-Rad reagent according to the supplier's instructions, and approximately 22 to 24 μg of protein was loaded in each lane. The molecular mass of the observed band is shown on the right side of the blot (64 kDa).

mants and the wild-type untransformed strain AX2 exhibited comparable generation times within a range from 9 to 13 h. Table 2 shows the generation time from one representative experiment for each transformant. The development of these *Dictyostelium* transformants in response to starvation was also similar to that of wild-type cells (unpublished data). The results indicate that the expression and import of mitochondrially targeted GFPs has no significant adverse effect on the expression and import of native mitochondrial proteins. To verify directly if this is so, we examined the levels of a representative nucleus-encoded mitochondrial protein, the catalytic subunit of succinate dehydrogenase (SdhA). The mature form (64 kDa) of *Dictyostelium* SdhA appeared at similar levels in AX2 and in all GFP transformants (regardless of the expression of either targeted or nontargeted GFP) both in whole-cell extracts (Fig. 7) and in mitochondrial extracts (data not shown). There is, therefore, no evidence that the targeted forms of GFP either saturate mitochondrial import channels or limit the rate of import or synthesis of other mitochondrial proteins. We conclude that the import-associated translational inhibition we observe is specific to the GFP itself and does not reflect a general impairment of expression or import of mitochondrial proteins.

## DISCUSSION

Much of our current understanding of the process of mitochondrial protein import has been generated by widely used in vitro import reactions due to their experimental flexibility and relative simplicity. Nearly all studies on mitochondrial protein import have been performed on in vitro systems, which have contributed enormously in defining the import apparatus. In these in vitro import reactions, purified or in vitro-synthesized precursor proteins are added to isolated mitochondria in a reaction mixture made as comparable as possible to the intracellular environment. However, these extracellular import systems do not truly represent the intracellular environment, as many unknown factors or parameters are likely to be missing in these systems. Most importantly, the consequences of cotranslational import are completely absent in most in vitro reactions which, by virtue of their design, are biased for posttranslational import. The fact that a precursor protein can be imported in vitro into mitochondria in a posttranslational manner does not preclude it from being imported cotranslationally in vivo. It should be borne in mind that the intracellular environment is structurally and compositionally much more complex than in vitro systems so that precursor proteins may be expected to behave differently in vivo.

Mitochondrial protein import is initiated by interaction of the N terminus of the polypeptide with the import apparatus in the mitochondrial outer membrane (33). It has been suggested that, in principle, such interaction can take place as soon as the nascent N terminus becomes available in the proximity of the import apparatus. If the precursor synthesis continues in close proximity with the mitochondria, then protein import can be initiated long before protein synthesis is complete, i.e., the import is likely to proceed in a cotranslational rather than posttranslational manner. It has been proposed that, in the highly structured intracellular environment of eukaryotic cells, mitochondrial protein synthesis actually takes place in localized domains close to the mitochondria rather than on free ribosomes in the cytoplasm (40). It may be a more energy-consuming process for cells to transport precursor proteins to the mitochondria, and it has also been suggested that some mitochondrial proteins can only be imported into mitochondria in a cotranslational manner, as the posttranslational import may be unachievable or less efficient due to the nature of the protein. Fumarase, the Krebs cycle enzyme, is a good example of a precursor protein which needs to be imported cotranslationally (21). In in vitro import systems, the precursor of fumarase cannot be successfully imported due to the rapid folding of the protein. The precursor protein becomes trapped in the import channel in vitro after the processing of the N-terminal end while the major part of the polypeptide stays outside the channel in a folded conformation. In vivo, this processed and folded polypeptide is released from the channel and remains active in the cytosol. Interestingly, the fumarase precursor was efficiently imported into mitochondria in a coupled translation-import reaction (reviewed in reference 24).

Our results suggest that the import of GFP fusion proteins into mitochondria also occurs cotranslationally in *D. discoideum* in vivo. Based on a comparative study of mitochondrially targeted and nontargeted GFP fusions proteins, our results demonstrate that the abundance of targeted GFP fusion proteins is restricted by a limited translation rate. Our observation suggests a novel phenomenon for mitochondrially targeted proteins: import-associated translational inhibition, in which the translational limitation appears to be a consequence of a cotranslational import into mitochondria. The inhibition was restricted to the mitochondrially targeted GFP itself and did not interfere with the import of other mitochondrial proteins in the same cell, with the result that growth rates and the expression of a representative mitochondrial protein, SdhA, were both unaffected.

In support of the conclusion that mitochondrially targeted GFP is imported cotranslationally, we found a strong association of GFP mRNA with the mitochondrial surface. Elucidation of the mechanism of mRNA localization at the mitochondrial surface has recently begun, and the mRNA has been found to be transported to its target in the form of a large ribonucleoprotein complex which contains a large number of

mRNAs and proteins (see reference 17 for a review). A *cis*-acting targeting signal for some mRNAs, which is conserved from yeast to humans, has been shown to reside in the 3′ UTR (38). This targeting sequence has the ability to target an otherwise nonlocalized mRNA to the mitochondria (see reference 17 for a review). We found in this work that aequorin mRNA did not associate with the mitochondria while the GFP mRNA did, regardless of the presence or absence of an import-competent leader peptide sequence. Since the only difference between our GFP constructs and corresponding aequorin constructs is the protein coding sequence, our results indicate the presence of an mRNA targeting signal within the GFP coding sequence.

The presence of an mRNA targeting signal in the GFP mRNA must be serendipitous, since GFP is not a native mitochondrial protein. In *S. cerevisiae*, it has been shown that a conserved sequence in the 3′ UTR of a number of mRNAs is responsible for targeting the mRNA to the mitochondrial surface. In the case of one of these, *ATP2*, the targeting signal has been localized experimentally to a 101-nucleotide region (nucleotides 50 to 150) and ascribed to a 70-nucleotide stem-loop structure in this region (27) (Fig. 8). To determine whether any serendipitous sequence identity existed between this targeting signal and the GFP or aequorin coding sequences, we performed *lfasta* (32) sequence alignments using 232 nucleotides of the *ATP2* 3′ UTR and the complete coding sequence of each of the two test proteins. We found no significant alignments with the aequorin sequence, but the first 67 nucleotides of GFP shared 56.2% identity with nucleotides 65 to 137 of the *ATP2* 3′ UTR. The *mfold* program (45) predicted a long stem-loop structure for the first 100 coding nucleotides of the GFP mRNA that exhibits striking similarities with the predicted secondary structure of the *ATP2* mRNA targeting signal (Fig. 8). We also used the FOLDALIGN (16) server (http://foldalign.kvl.dk) to search for significant local RNA structural alignments between nucleotides 50 to 150 of the *ATP2* 3′ UTR and the GFP and aequorin mRNA coding sequences. In addition to the 5′ stem-loop already identified, we found by this means two additional long stem-loops in the middle and near the 3′ end of the GFP mRNA (Fig. 8). However, we found no similar, long stem-loops in the aequorin mRNA coding sequence. These results suggest that the GFP but not the aequorin mRNA may mimic in up to three places the secondary structure of a conserved targeting signal that directs the mRNA of some mitochondrial proteins to the mitochondrial surface. It would be of interest in future studies to verify whether one or more of these stem-loops is sufficient to direct passenger mRNA molecules to the mitochondrial surface in *Dictyostelium*.

Having found its way to the mitochondrial surface, the GFP mRNA is translated at a rate that depends upon whether the encoded polypeptide is imported or not. There are at least three ways in which import could limit the rate of translation. Firstly, during cotranslational import, the rate of translocation of the nascent polypeptide through the import pore may directly limit the rate of polypeptide extension and release from the ribosome. Secondly, the number of active translational complexes may be limited by the availability of import channels. This situation would be analogous to cotranslational translocation into the endoplasmic reticulum (ER), where it

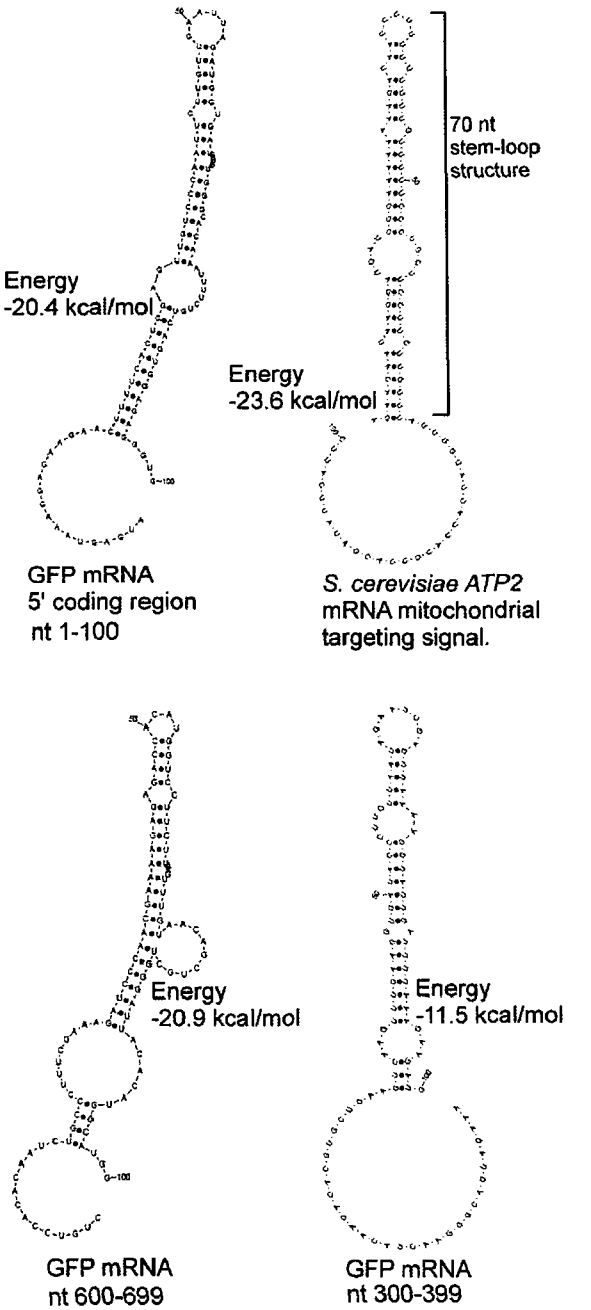


FIG. 8. Comparison of predicted secondary structures of the *Saccharomyces cerevisiae ATP2* mRNA mitochondrial targeting signal and sections of the GFP mRNA. Regions of sequence and/or structural similarity between the *ATP2* 3′ UTR and the GFP mRNA were found using the *lfasta* program (32) and the FOLDALIGN web server (http://foldalign.kvl.dk/server/index.html). The Burnet Institute Mfold Server (http://mfold.burnet.edu.au/) was used to predict secondary structures for stretches of 100 bases containing the aligned regions: nucleotides (nt) 50 to 149 of the 3′ untranslated region of the *S. cerevisiae ATP2* mRNA and nucleotides 1 to 100, 300 to 399, and 600 to 699 of the GFP mRNA.

was previously shown that the elongation of the polypeptide chain is delayed or arrested until the nascent peptide-ribosome complex interacts with the docking protein (SRP receptor) on the ER membrane (12, 29). Similar translational arrest may be expected for cotranslational translocation into the mitochondria if the interaction between the NAC complex and the mitochondrial import apparatus is delayed or infrequent. A third possible explanation for the translational inhibition observed in this report is that polypeptide synthesis contributes to the driving force for import so that synthesis is less energetically favorable. As the SRP receptor and a complex (Sec61p complex) on the ER membrane are sufficient for translocation of preproteins (14), it has been speculated that the major driving force for cotranslational import into the ER might come from the elongation of the polypeptide chain on the ribosome (28). If the elongation process is exploited to contribute driving force for cotranslational import, then the process of elongation (synthesis) during cotranslational import is expected to be suppressed compared to the synthesis on free cytosolic ribosomes. Our results do not allow us to distinguish between these various mechanisms for import-associated translational inhibition, nor do they reveal whether the translation of native mitochondrial proteins expressed under the control of their endogenous promoters is ever limited by the import process.

Regardless of whether import-associated inhibition of translation is physiologically relevant to normal mitochondrial biogenesis, its occurrence in the GFP case in this study and the association of the GFP mRNA with the mitochondrial surface have revealed that mitochondrial protein import can be cotranslational. That the same phenomena did not occur with otherwise identical constructs encoding a different test protein (aequorin) suggests that whether or not import proceeds cotranslationally depends upon whether or not the mRNA itself is targeted to the mitochondrial surface. It would be of interest to determine in microarray studies which of the endogenous mitochondrial proteins in *Dictyostelium* are encoded on mitochondrially targeted mRNAs. Such experiments in yeast led to the suggestion that the mitochondrially targeted mRNAs are those that encode mitochondrial proteins of ancient bacterial origin derived from the original protomitochondrial ancestor (26).

## ACKNOWLEDGMENTS

A.U.A. was a recipient of a La Trobe University Postgraduate Research Award. S.T.L. was a recipient of an Australian Postgraduate Research Award.

## REFERENCES

1. **Ades, I. Z., and R. A. Butow.** 1980. The transport of proteins into yeast mitochondria. Kinetics and pools. J. Biol. Chem. **255**:9925–9935.
2. **Barth, C., U. Greferath, M. Kotsifas, and P. R. Fisher.** 1999. Polycistronic transcription and editing of the mitochondrial small subunit (SSU) ribosomal RNA in Dictyostelium discoideum. Curr. Genet. **36**:55–61.
3. **Brix, J., K. Dietmeier, and N. Pfanner.** 1997. Differential recognition of preproteins by the purified cytosolic domains of the mitochondrial import receptors Tom20, Tom22, and Tom70. J. Biol. Chem. **272**:20730–20735.
4. **Chambers, J. M.** 1998. Programming with data. Springer, New York, N.Y.
5. **Corral-Debrinski, M., C. Blugeon, and C. Jacq.** 2000. In yeast, the 3′ untranslated region or the presequence of ATM1 is required for the exclusive localization of its mRNA to the vicinity of mitochondria. Mol. Cell. Biol. **20**:7881–7892.
6. **Fey, P., K. Compton, and E. C. Cox.** 1995. Green fluorescent protein production in the cellular slime molds Polysphondylium pallidum and Dictyostelium discoideum. Gene **165**:127–130.
7. **Fujiki, M., and K. Verner.** 1993. Coupling of cytosolic protein synthesis and mitochondrial protein import in yeast. Evidence for cotranslational import in vivo. J. Biol. Chem. **268**:1914–1920.
8. **Fujiki, M., and K. Verner.** 1991. Coupling of protein synthesis and mitochondrial import in a homologous yeast in vitro system. J. Biol. Chem. **266**:6841–6847.
9. **Funfschilling, U., and S. Rospert.** 1999. Nascent polypeptide-associated complex stimulates protein import into yeast mitochondria. Mol. Biol. Cell **10**:3289–3299.
10. **Gautschi, M., H. Lilie, U. Funfschilling, A. Mun, S. Ross, T. Lithgow, P. Rucknagel, and S. Rospert.** 2001. RAC, a stable ribosome-associated complex in yeast formed by the DnaK-DnaJ homologs Ssz1p and zuotin. Proc. Natl. Acad. Sci. USA **98**:3762–3767.
11. **George, R., T. Beddoe, K. Landl, and T. Lithgow.** 1998. The yeast nascent polypeptide-associated complex initiates protein targeting to mitochondria in vivo. Proc. Natl. Acad. Sci. USA **95**:2296–2301.
12. **Gilmore, R., P. Walter, and G. Blobel.** 1982. Protein translocation across the endoplasmic reticulum. II. Isolation and characterization of the signal recognition particle receptor. J. Cell Biol. **95**:470–477.
13. **Gilson, P. R., X. C. Yu, D. Hereld, C. Barth, A. Savage, B. R. Kiefel, S. Lay, P. R. Fisher, W. Margolin, and P. L. Beech.** 2003. Two Dictyostelium orthologs of the prokaryotic cell division protein FtsZ localize to mitochondria and are required for the maintenance of normal mitochondrial morphology. Eukaryot. Cell **2**:1315–1326.
14. **Gorlich, D., and T. A. Rapoport.** 1993. Protein translocation into proteoliposomes reconstituted from purified components of the endoplasmic reticulum membrane. Cell **75**:615–630.
15. **Harmey, M. A., G. Hallermayer, H. Korb, and W. Neupert.** 1977. Transport of cytoplasmically synthesized proteins into the mitochondria in a cell free system from *Neurospora crassa*. Eur. J. Biochem. **81**:533–544.
16. **Havgaard, J. H., R. B. Lyngsø1, and J. Gorodkin.** 2005. The FOLDALIGN web server for pairwise structural RNA alignment and mutual motif search. Nucleic Acids Res. **33**:W650–W653.
17. **Jansen, R. P.** 2001. mRNA localization: message on the move. Nat. Rev. Mol. Cell Biol. **2**:247–256.
18. **Kellems, R. E., V. F. Allison, and R. A. Butow.** 1975. Cytoplasmic type 80S ribosomes associated with yeast mitochondria. IV. Attachment of ribosomes to the outer membrane of isolated mitochondria. J. Cell Biol. **65**:1–14.
19. **Kellems, R. E., and R. A. Butow.** 1972. Cytoplasmic-type 80 S ribosomes associated with yeast mitochondria. I. Evidence for ribosome binding sites on yeast mitochondria. J. Biol. Chem. **247**:8043–8050.
20. **Kellems, R. E., and R. A. Butow.** 1974. Cytoplasmic type 80 S ribosomes associated with yeast mitochondria. 3. Changes in the amount of bound ribosomes in response to changes in metabolic state. J. Biol. Chem. **249**:3304–3310.
21. **Knox, C., E. Sass, W. Neupert, and O. Pines.** 1998. Import into mitochondria, folding and retrograde movement of fumarase in yeast. J. Biol. Chem. **273**:25587–25593.
22. **Komori, K., F. Maruo, T. Morio, H. Urushihara, and Y. Tanaka.** 1997. Localization of a DNA topoisomerase II to mitochondria in *Dictyostelium discoideum*: deletion mutant analysis and mitochondrial targeting signal presequence. J. Plant Res. **110**:65–75.
23. **Kotsifas, M., C. Barth, A. de Lozanne, S. T. Lay, and P. R. Fisher.** 2002. Chaperonin 60 and mitochondrial disease in Dictyostelium. J. Muscle Res. Cell Motil. **23**:839–852.
24. **Lithgow, T.** 2000. Targeting of proteins to mitochondria. FEBS Lett. **476**:22–26.
25. **Maccecchini, M. L., Y. Rudin, G. Blobel, and G. Schatz.** 1979. Import of proteins into mitochondria: precursor forms of the extramitochondrially made F1-ATPase subunits in yeast. Proc. Natl. Acad. Sci. USA **76**:343–347.
26. **Marc, P., A. Margeot, F. Devaux, C. Blugeon, M. Corral-Debrinski, and C. Jacq.** 2002. Genome-wide analysis of mRNAs targeted to yeast mitochondria. EMBO Rep. **3**:159–164.
27. **Margeot, A., C. Blugeon, J. Sylvestre, S. Vialette, C. Jacq, and M. Corral-Debrinski.** 2002. In *Saccharomyces cerevisiae*, ATP2 mRNA sorting to the vicinity of mitochondria is essential for respiratory function. EMBO J. **21**:6893–6904.
28. **Mayer, A., W. Neupert, and R. Lill.** 1995. Mitochondrial protein import: reversible binding of the presequence at the trans side of the outer membrane drives partial translocation and unfolding. Cell **80**:127–137.
29. **Meyer, D. I., E. Krause, and B. Dobberstein.** 1982. Secretory protein translocation across membranes-the role of the "docking protein'. Nature **297**:647–650.
30. **Nebl, T., and P. R. Fisher.** 1997. Intracellular Ca2+ signals in Dictyostelium chemotaxis are mediated exclusively by Ca2+ influx. J. Cell Sci. **110**(Pt 22):2845–2853.
31. **Ni, L., T. S. Heard, and H. Weiner.** 1999. In vivo mitochondrial import. A comparison of leader sequence charge and structural relationships with the in vitro model resulting in evidence for co-translational import. J. Biol. Chem. **274**:12685–12691.
32. **Pearson, W. R., and D. J. Lipman.** 1988. Improved tools for biological sequence comparison. Proc. Natl. Acad. Sci. USA **85**:2444–2448.

33. **Pfanner, N., and A. Geissler.** 2001. Versatility of the mitochondrial protein import machinery. Nat. Rev. Mol. Cell Biol. **2**:339–349.
34. **Pfanner, N., and K. N. Truscott.** 2002. Powering mitochondrial protein import. Nat. Struct. Biol. **9**:234–236.
35. **Reid, G. A., and G. Schatz.** 1982. Import of proteins into mitochondria. Yeast cells grown in the presence of carbonyl cyanide m-chlorophenylhydrazone accumulate massive amounts of some mitochondrial precursor polypeptides. J. Biol. Chem. **257**:13056–13061.
36. **Roise, D., and G. Schatz.** 1988. Mitochondrial presequences. J. Biol. Chem. **263**:4509–4511.
37. **Roise, D., F. Theiler, S. J. Horvath, J. M. Tomich, J. H. Richards, D. S. Allison, and G. Schatz.** 1988. Amphiphilicity is essential for mitochondrial presequence function. EMBO J. **7**:649–653.
38. **Sylvestre, J., A. Margeot, C. Jacq, G. Dujardin, and M. Corral-Debrinski.** 2003. The role of the 3′ untranslated region in mRNA sorting to the vicinity of mitochondria is conserved from yeast to human cells. Mol. Biol Cell. **14**:3848–3856.
39. **Troll, H., T. Winckler, I. Lascu, N. Muller, W. Saurin, M. Veron, and R. Mutzel.** 1993. Separate nuclear genes encode cytoplasmic and mitochondrial nucleoside diphosphate kinase in Dictyostelium dicoideum. J. Biol. Chem. **268**:25469–25475.
40. **Verner, K.** 1993. Co-translational protein import into mitochondria: an alternative view. Trends Biochem. Sci. **18**:366–371.
41. **von Heijne, G.** 1992. Cleavage-site motifs in protein targeting sequences. Genet. Eng. **14**:1–11.
42. **von Heijne, G.** 1986. Mitochondrial targeting sequences may form amphiphilic helices. EMBO J. **5**:1335–1342.
43. **Wiedmann, B., H. Sakai, T. A. Davis, and M. Wiedmann.** 1994. A protein complex required for signal-sequence-specific sorting and translocation. Nature **370**:434–440.
44. **Wienhues, U., K. Becker, M. Schleyer, B. Guiard, M. Tropschug, A. L. Horwich, N. Pfanner, and W. Neupert.** 1991. Protein folding causes an arrest of preprotein translocation into mitochondria *in vivo*. J. Cell Biol. **115**:1601–1610.
45. **Zuker, M.** 1989. On finding all suboptimal foldings of an RNA molecule. Science **244**:48–52.